



## Relationship between cloud-to-ground discharge and penetrative clouds: A multi-channel satellite application

Luiz A.T. Machado <sup>a,\*</sup>, Wagner F.A. Lima <sup>a</sup>, Osmar Pinto Jr. <sup>a</sup>, Carlos A. Morales <sup>b</sup>

<sup>a</sup> Instituto Nacional de Pesquisas Espaciais, Rodovia Pres. Dutra, km 40, Cachoeira Paulista/SP-12630-000, Brazil

<sup>b</sup> Instituto de Astronomia, Geofísica e Ciências Atmosféricas., Rua do Matão, 1226-Cidade Universitária-Sao Paulo/SP-05508-090, Brazil

### ARTICLE INFO

#### Article history:

Received 29 November 2007

Received in revised form 20 August 2008

Accepted 6 October 2008

#### Keywords:

Lightning

Penetrative clouds

### ABSTRACT

This work presents a relationship between atmospheric cloud-to-ground discharges and penetrative convective clouds. It combines Infrared and Water Vapor channels from the GOES-12 geostationary satellite with cloud-to-ground discharge data from the Brazilian Integrated Lightning Detection Network (RINDAT) during the period from January to February 2005. The difference between water vapor and infrared brightness temperature is a tracer penetrating clouds. Due to the water vapor channel's strong absorption, this difference is positive only during overshooting cases, when convective clouds penetrate the stratosphere. From this difference and the cloud-to-ground discharge measured on the ground by RINDAT, it was possible to adjust exponential curves that relate the brightness temperature difference from these two channels to the probability of occurrence of cloud-to-ground discharges, with a very large coefficient of determination. If WV-IR brightness temperature difference is greater than  $-15$  K there is a large potential for cloud-to-ground discharge activity. As this difference increases the cloud-to-ground discharge probably increases, for example: if this difference is equal to zero, the probability of having at least one cloud-to-ground discharge is 10.9%, 7.0% for two, 4.4% for four, 2.7% for eight and 1.5% for sixteen cloud-to-ground discharges. Through this process, was developed a scheme that estimates the probability of occurrence of cloud-to-ground discharge over all the continental region of South America.

© 2008 Elsevier B.V. All rights reserved.

### 1. Introduction

Multispectral satellite analysis has demonstrated its ability to depict cloud top features. The combination of water vapor and infrared window channels to describe deep convective clouds has been largely used; for instance, [Medaglia et al. \(2005\)](#) used these channels from geostationary satellites to develop the Global Convective Diagnostic. [Schmetz et al. \(1997\)](#) noted through simultaneous observation of the METEOSAT infrared window and water vapor channels and a line-by-line radiative transfer model that differences greater

than zero degrees between both channels are related to convective clouds with high vertical extension. The simulations show that the larger brightness temperatures in the water vapor channel are due to stratospheric water vapor, which absorbs radiation from overshooting tops and emits radiation at a higher stratospheric temperature. [Adler and Mack \(1986\)](#) studying the cloud top dynamics also found storm tops above the tropopause. [Fritz and Laszlo \(1993\)](#) also noted a brightness temperature from the water vapor channel warmer than from the infrared window channel over a region associated with deep convection. [Kurino \(1997\)](#) showed that the difference between both brightness temperatures can be very useful in defining heavy precipitation related to deep convection. [Reudenbach et al. 2001](#) use this difference to discriminate deep convection from thick Cirrus clouds. [Stevak et al. \(2007\)](#) used the higher spatial resolution images from the MODIS sensor to investigate the correlation between

\* Corresponding author. Instituto Nacional de Pesquisas Espaciais, Centro de Previsão de Tempo e Estudos Climáticos, Divisão de Satélites e Sistemas Ambientais, Rodovia Pres. Dutra, km 40, Cachoeira Paulista/SP-12630-000, Brazil. Tel.: +55 12 31869399; fax: +55 12 31869291.

E-mail address: [luiz.machado@cptec.inpe.br](mailto:luiz.machado@cptec.inpe.br) (L.A.T. Machado).

cloud top temperature and the water vapor-infrared window difference. They consider that a positive difference is possible if each storm top generates some amount of moisture in the stratosphere, or by pre-existent stratospheric moisture in a layer above the cloud top. They found some cases that agree with the previous results, where the positive difference is well correlated with the minimal cloud top temperature. However, one case did not agree; the larger difference was not correlated with the minimal temperature. They also suggest that different ice emissivity for each channel can in some cases explain these differences. Wang (2007), using a three-dimensional non-hydrostatic cloud model studied penetrating convective clouds. He suggests that moisture plumes in the stratosphere above convective clouds are generated by gravity waves and large instability over the cloud top due to convection inside the storm.

The main goal of this study is to test the hypotheses that the difference between the water vapor and infrared channel can be used as a tracer of penetrative clouds, and those clouds are related to cloud-to-ground discharge.

Section 2 describes the data and the methodology employed in this study. Section 3 presents the results obtained, comparing satellite data and cloud-to-ground discharge occurrence, and finally Section 4 presents the conclusion.

## 2. Methodology

Schmetz et al. (1997) suggested that positive differences between water vapor and infrared brightness temperature are only possible when deep convective clouds penetrate in the tropopause, moistening the stratosphere. The infrared is located in the window channel; a region of the electromagnetic spectrum where the earth atmosphere's slightly absorbs

terrestrial radiation. However, the water vapor channel has strong absorption features and the brightness temperature reported by this channel is nearly always colder than that measured in the infrared channel. Therefore, the difference between the water vapor and infrared window channels is normally negative, except if penetrating clouds go through the tropopause, moistening the stratosphere and then, as the temperature increases in this layer, the difference can be positive. In these cases, these positive differences are related to overshooting, which is normally associated with high deep convective cloud tops with a large amount of ice, chiefly responsible for the development of an electrical field inside the clouds. The atmospheric cloud-to-ground discharges are the response of the accumulated charges inside the cloud that can breakdown the dielectric air (Pinto et al., 2004). The center of charges (positive and negative) is formed by several cloud microphysical processes that transfer positive and negative charges during the formation of cloud droplets, rain drops and ice particles (MacGorman and Rust, 1998). Moreover, observational studies revealed that lightning is associated with glaciation, and the flash rate increases as the volume of precipitation-sized ice particles in the mixed-phase region increases and updraft strengthens (Baker et al., 1995; Petersen and Rutledge, 1998). The mixed phase clouds were observed to occur occasionally up to the homogeneous ice nucleation and cloud electrification processes can extend up to the higher levels of the clouds (Heysfield and Miloshevich, 1993).

Therefore, these very deep and high extended clouds are responsible for a very large rate of cloud-to-ground discharges (Abdoulav et al., 2001). The difference between these two brightness temperatures can be used as a proxy for very deep convection cases (overshooting cases) associated with frequent lightning. Considering these features, we will

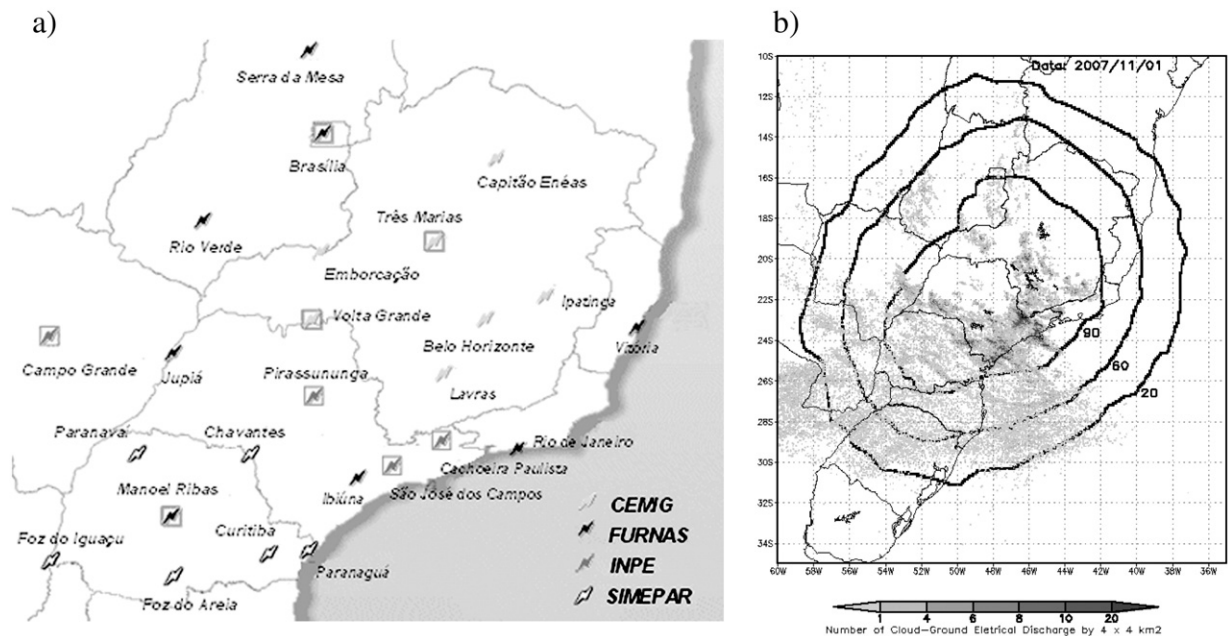


Fig. 1. a) Location of RINDAT sensors and the institution responsible for each sensor. b) Number of cloud-to-ground discharges per day on November 1st 2007, and lightning detection efficiency contour lines within the 20, 60, and 90%.

combine satellite with cloud-to-ground discharge data to check this hypothesis and quantify this relationship.

### 2.1. The RINDAT network

RINDAT is a cloud-to-ground lightning detection network covering the south and southeast parts of Brazil. The RINDAT operates at LF/VLF, with an average sensor baseline of 300 km. It is a consortium of Brazilian electricity companies and research institutes. RINDAT technology is based on LPATS (Lightning Position and Tracking System) and IMPACT (Improved Accuracy Using Combined Technology) sensors for locating lightning sources at medium and long ranges. More details about RINDAT can be found in Pinto (2003). During the period analyzed, the network was composed of 24 sensors (8 Impact and 16 LPATS sensors), as indicated in Fig. 1a. Data from the sensors are sent to a central processor where they are disseminated and stored and later reprocessed to recover data losses from possible delays in communication links. The data employed in this study consist of time and location of the cloud-to-ground electrical discharges from January to February 2005. RINDAT is able to locate cloud-ground discharges with an average location accuracy of 500 m for flashes occurring inside the network. Fig. 1b shows the detection efficiency contours. This work used only the information for Sao Paulo State that is inside the area with detection efficiency higher than 90%.

### 2.2. GOES 12

The infrared (IR) 10.2–11.2  $\mu\text{m}$  and the water vapor (WV) 6.5–7.0  $\mu\text{m}$  channels from GOES-12 were employed to calculate the penetrating clouds. The data employed in this

study were images (Full Disk, Northern Hemisphere Extended and Southern Hemisphere) available every 30 min covering the period from January to February 2005. IR and WV channels have the same resolution (4 km at the subsatellite point) and projection, therefore the overlay is straightforward and the difference between the channels is easily performed. We have used full resolution images in the satellite projection to perform the channel differences. The time of each image normally corresponds to the time of the first image scan line. In this work we did not use the image time but the specific time of each scan line to combine precisely with the cloud-to-ground discharge.

### 2.3. Probability of occurrence

Inside the 90% lightning detection efficiency region we applied the following methodology: For each image pixel difference (WV-IR) we searched for the occurrence of cloud-to-ground discharge reported by RINDAT, 7.5 min before or after the time of the scan line, in a region with a 10 km radius centered on the pixel position. Fig. 1b shows an example of the number of cloud-to-ground discharge per pixel for one day within the 20, 60, and 90% detection efficiency contour lines.

Statistical analysis was performed for the WV-IR differences in the temperature interval between  $-15\text{ K}$  to  $+3\text{ K}$ . This interval was chosen considering the significant lightning occurrence observed in the dataset. This information was separated in 1-deg intervals and the total number of cloud-to-ground discharge occurrences computed, the amount of time when at least  $j$  cloud-to-ground discharge occurred ( $LD_i^j$ —occurrence in the WV-IR bin interval  $i$ ) and the amount of time that no cloud-to-ground discharge was reported ( $NLD_i$ —no occurrence in the WV-IR bin interval  $i$ ).

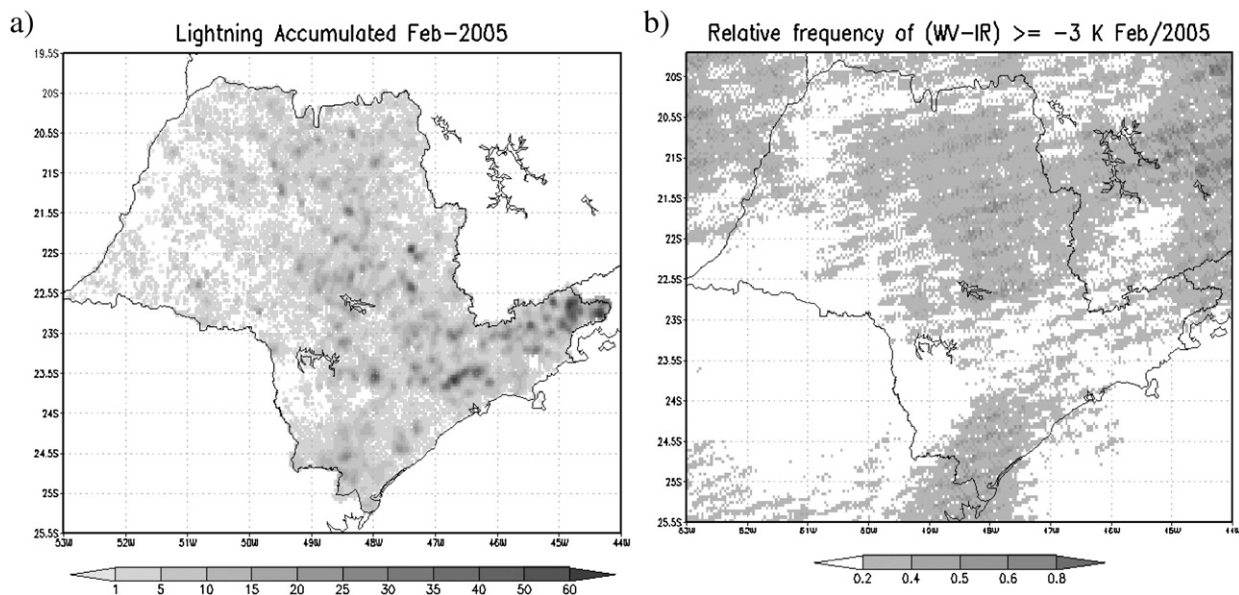


Fig. 2. a) Spatial distribution of the cloud-to-ground discharges occurring February 2005 in Sao Paulo State. b) Spatial distribution of the relative frequency of WV-IR brightness temperature differences greater than  $-3\text{ K}$ , in February 2005 in Sao Paulo State.

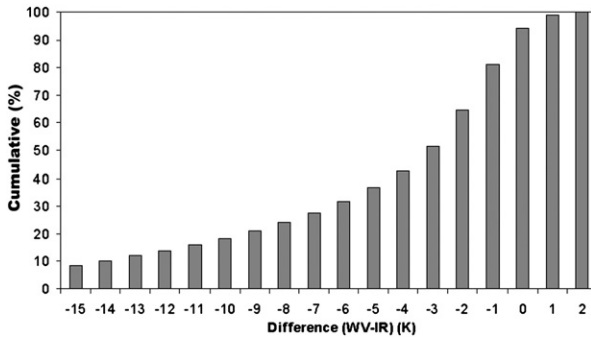


Fig. 3. Cumulative frequency (%) of cloud-to-ground discharge occurrence as a function of the WV-IR brightness temperature (K).

The probability to have at least  $j$  cloud-to-ground discharge occurrence  $P_i(\geq j)$  for each temperature bin interval ( $i$ ) was defined as

$$P_i(\geq j) = \frac{LD_j}{LD_j + NLD_i} \quad (1)$$

Inside the region analyzed we reported 189,577 cloud-to-ground discharge occurrences, 119,703 in January and 69,874 in February.

### 3. Results

We have focused the analyses of cloud-to-ground discharge occurrences over the State of Sao Paulo, where RINDAT has 90% flash detection efficiency. We also computed the frequency of occurrence of WV-IR differences greater than  $-3$  K. This threshold was used because it corresponds to the WV-IR brightness temperature difference in which 50% of lightning cases occur (see Fig. 3). Fig. 2a shows the spatial distribution of monthly cloud-to-ground discharge occurrences during February of 2005 (the grid corresponds to a Cartesian projection spaced by  $0.04^\circ$ ). Fig. 2b presents the spatial distribution, at the same projection, of the relative frequency (one corresponds to the maximum occurrence) of the WV-IR greater than  $-3$  K. The majority of lightning occurs in the eastern region of the Sao Paulo State, around large cities, such as Sao Paulo, and near the orographic region. The interesting result, however, is the similarity of WV-IR spatial distribution and lightning occurrence, showing that this difference is well connected to penetrative clouds and consequently associated with cloud-to-ground discharge.

Fig. 3 shows cloud-to-ground discharge cumulative frequency of occurrence as a function of the WV-IR brightness temperature difference. It is noted that only 8.4% of cloud-to-ground discharge occurs for WV-IR smaller than  $-15$  K and 99.9% occurs for WV-IR values smaller than 2 K. The 8.4% of lightning cases take place over a large interval of WV-IR smaller than  $-15$  K. 50% of cloud-to-ground discharge occurs when WV-IR is greater than  $-3$  K. This result shows that the combination of these two channels is well associated with thunderstorm activity and consequently cloud electrical activity.

The occurrence probabilities for at least one, two, four, eight and sixteen cloud-to-ground discharge as a function of

the WV-IR brightness difference was computed using Eq. (1). We found an exponential increase in lightning's probability of occurrence as the WV-IR difference increases. Fig. 4 shows the relative frequency of occurrence for different values of lightning occurrence as a function of the WV-IR difference. For instance, for the WV-IR difference equal to zero, the probability of cloud-to-ground discharge is equal to 10.9%, 7.0%, 4.4%, 2.7% and 1.5% for at least one, two, four, eight and sixteen cloud-to-ground discharges respectively. The probability of having more than sixteen cloud-to-ground discharges in 15 min only occurs for a WV-IR difference greater than  $-4$  K, otherwise it is zero. Due to a strong decrease in the number of cases of WV-IR differences greater than 3 K we have computed the differences up to this value. For 3 K differences, the probability of having cloud-to-ground discharge is 18.6%, 13.2%, 8.6%, 3.7% and 1.2% for at least one, two, four, eight and sixteen cloud-to-ground discharges respectively. The probability values are quite small if compared with the cloud-to-ground discharge occurrence as a function of WV-IR difference, it is related to the considerable number of cases when WV-IR difference is high and no discharge is observed. We can note that eight and sixteen lightning occurrences inside the 15-minute interval for WV-IR equal to 3 K are slightly smaller than for 2 K, it is probably due to small amount of cases reporting for 3 K.

It was possible to adjust an exponential curve that relates WV-IR difference to probability of occurrence of a given number of cloud-to-ground discharges, with a large coefficient of determination around 0.9, as shown by Eq. (2). Fig. 4 also shows the adjusted exponential curves for each case of cloud-to-ground discharge occurrence.

$$\begin{aligned} P_i(\geq 1) &= 9.3 * \exp(0.19 * i) \\ P_i(\geq 2) &= 6.2 * \exp(0.21 * i) \\ P_i(\geq 4) &= 3.9 * \exp(0.21 * i) \\ P_i(\geq 8) &= 2.2 * \exp(0.21 * i) \\ P_i(\geq 16) &= 1.0 * \exp(0.21 * i) \end{aligned} \quad (2)$$

Where, ( $i$ ) corresponds to the WV-IR brightness temperature difference in Kelvin.

Based on this result and considering that the statistical results obtained in this study can be extrapolated to a larger

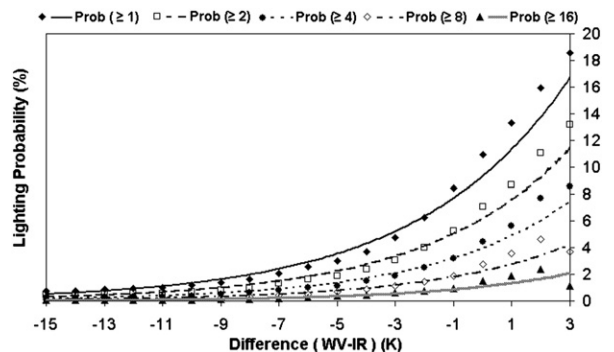
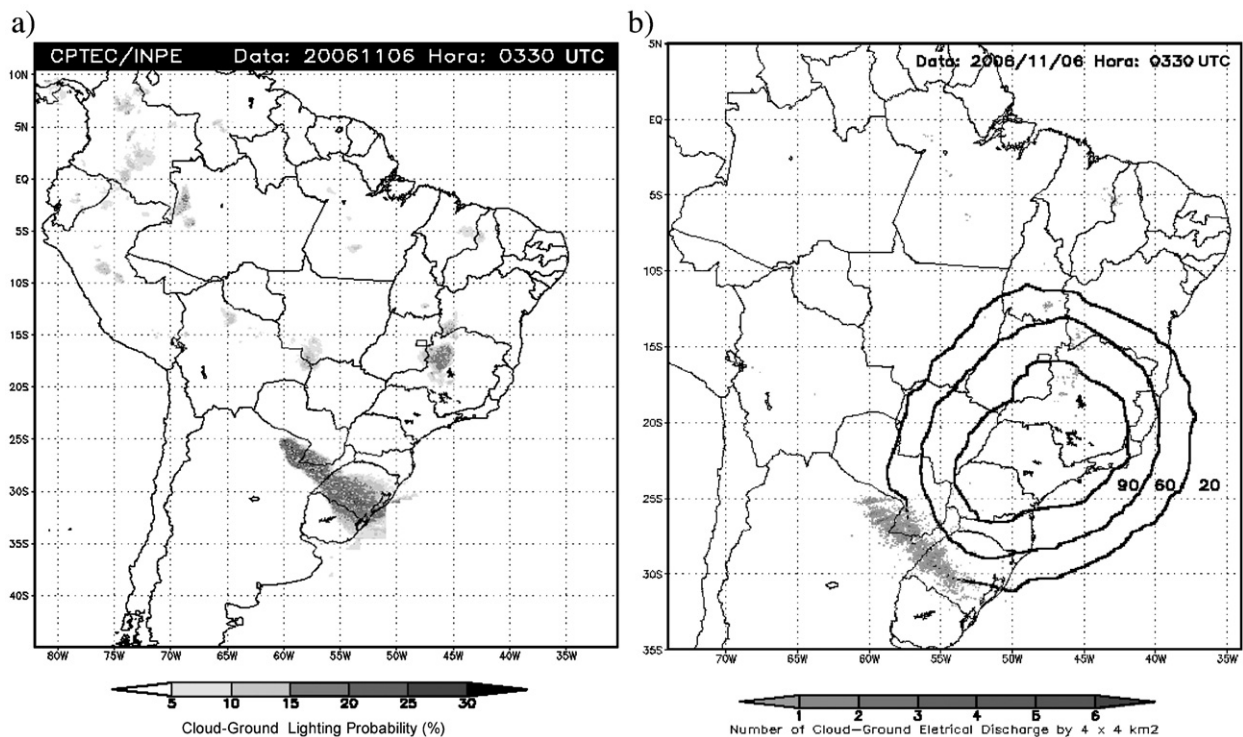


Fig. 4. Frequency of occurrence and adjusted exponential curves of cloud-to-ground discharge as a function of the WV-IR brightness temperature difference for the probability of having at least one, two, four, eight and sixteen cloud-to-ground discharges in 15-minute intervals.



**Fig. 5.** a) Probability of lightning occurrence for November 6th 2006 at 03:30 GMT. b) Number of cloud-to-ground discharges per pixel 7.5 min before and after 03:30 GMT on the same day.

region, we estimate the probability of occurrence of cloud-to-ground discharge for all continental South America. But these remain to be validated; the verification of these assertions can only be evaluated when the RINDAT network has been improved with more sensors covering the other regions. Fig. 5 shows an example of the operational product, using GOES 12 images and the number of cloud-to-ground discharges per pixel in 15-minute intervals reported by the RINDAT network for the same time. We can note the similarity of the results even outside the region of large detection efficiency. For this case shown in Fig. 5 we have computed the probability of detection and false alarm. There were 7319 pixels with at least one cloud-to-ground discharge, 85.8% of these pixels had  $WV-IR > 0$  K, and the 14.2% remaining of the pixels had  $WV-IR < 0$ . The probability of detection is very high, however, the false alarm rate is also very high, this is the reason for the probability to have at least one cloud-to-ground discharge for  $WV-IR > 0$  K is only 10.9% (see Fig. 4). For this case the false alarm rate for  $WV-IR > 0$  is 74.9% however, for  $WV-IR > 5$  K is only 14.8%. The considerable reduction in the false alarm rate for larger  $WV-IR$  difference suggests that the lower  $WV-IR$  difference also includes the decay stage of the penetrative clouds when the updrafts is considerably reduced but the cloud top still remain penetrative.

#### 4. Conclusions

This study combines water vapor and infrared window channels to detect cloud-to-ground discharges. The  $WV-IR$  brightness temperature difference can be used as a proxy for

deep convection. We have found that values greater than  $-15$  K are associated with penetrative clouds with potential for cloud-to-ground discharge activity. As the brightness temperature difference increases, the probability of lightning increases. These differences are also associated with the probability to have a specific number of cloud-to-ground discharges per pixel. For instance, if this difference is equal to zero, the probability of having at least one cloud-to-ground discharge is 10.9%, 7.0% for two, 4.4% for four, 2.7% for eight and 1.5% for sixteen cloud-to-ground discharges. The probability of cloud-to-ground discharge can be expressed as an exponential function of the  $WV-IR$  brightness temperature difference.

The physical process behind these results is that  $WV-IR$  values greater than  $-15$  K are associated with deep convective clouds close to the tropopause or penetrating storm tops in the stratosphere (overshooting clouds). Thus, these clouds contain large amounts of ice and highly extended, therefore having a considerable potential for strong lightning activity. The probability of cloud-to-ground discharge as a function of the  $WV-IR$  difference is a combination of a high probability of detection and false alarm rate. Further studies should be made to investigate if additional information about cloud life stage can reduce the false alarm rate.

Based on these results it is possible to estimate the probability of cloud-to-ground discharge using GOES images over South America over the region not covered by the RINDAT network. This result should be tested over other continental regions to determine if the statistical results obtained over this region can be extrapolated to all other continental regions and seasons.

## Acknowledgements

We would like to thank RINDAT for providing the reprocessed data and NOAA for providing GOES satellite images. We acknowledge the review comments.

## References

- Abdoulbaev, S., Marques, V.S., Pinheiro, F.M.A., Martinez, E.F.A., Lenskaia, O., 2001. Analysis of mesoscale system using cloud-to-ground flash data. *Braz. J. Geophys.* 19 (1), 75–95.
- Adler, R.F., Mack, R.A., 1986. Thunderstorm cloud top dynamics as inferred from satellite observations and a cloud top parcel model. *J. Atmos. Sci.* 43 (18), 1945–1960.
- Baker, M.B., Christian, H.J., Latham, J., 1995. A computational study of the relationships linking lightning frequency and other thundercloud parameters. *Q. J. R. Meteorol. Soc.* 121, 1525–1548.
- Fritz, S., Laszlo, I., 1993. Detection of water vapor in the stratosphere over very high clouds in the tropics. *J. Geophys. Res.* 98 (D12), 22959–22967.
- Heymsfield, A.J., Miloshevich, L.M., 1993. Homogenous ice nucleation and supercooled liquid water in orographic wave clouds. *J. Atmos. Sci.* 50, 2335–2353.
- Kurino, T., 1997. A satellite infrared technique for estimating “Deep/Shallow” precipitation. *Adv. Space Res.* 19 (3), 511–514.
- MacGorman, D.R., Rust, W.D., 1998. *The Electrical Nature of Storms*. Oxford University Press, New York.
- Medaglia, C.M., Adamo, C., Formenton, M., Piccolo, F., 2005. Nowcasting of convective cells over Italian Peninsula. *Adv. Geosci.* 2, 173–176.
- Petersen, W.A., Rutledge, S.A., 1998. On the relationships between cloud-to-ground lightning and convective rainfall. *J. Geophys. Res. Atmos.* 103 (D12), 14025–14040.
- Pinto Jr., O., 2003. *The Brazilian Lightning Detection Network: A Historical Background and Future Perspectives*, Proceedings of VII International Symposium on Lightning Protection (SIPDA). Curitiba, Brazil.
- Pinto Jr., O., Saba, M.M.F., Pinto, I.R.C.A., Tavares, F.S.S., Solorzano, N.N., Naccarato, K.P., Taylor, M., Pautet, P.D., Holzworth, R.H., 2004. Thunderstorm and lightning characteristics associated with sprites in Brazil. *Geophys. Res. Lett.* 31 (13), 13103–13106.
- Reudenbach, C., Heinemann, G., Heuel, E., Bendix, J., Winiger, M., 2001. Investigation of summertime convective rainfall in Western Europe based on a synergy of remote sensing data and numerical models. *Meteor. Atmosph. Phys.* 76, 23–41.
- Schmetz, J., Tjemkes, S.A., Gube, M., Van de Berg, L., 1997. Monitoring deep convection and convective overshooting. *Adv. Space Res.* 19 (3), 433–441.
- Stevak, M., Rabin, R.M., Wang, P.K., 2007. Contribution of the MODIS instrument to observations of deep convective storms and stratospheric moisture detection in GOES and MSG imagery. *Atmos. Res.* 83, 505–518.
- Wang, P.K., 2007. The thermodynamic structure atop a penetrating convective thunderstorm. *Atmos. Res.* 83, 254–262.